

# Investigation of cell mismatch in three single crystalline silicon photovoltaic modules using Electroluminescence as a diagnostic technique

JL Crozier\*, FJ Vorster and EE van Dyk

Department of Physics, PO Box 77000, Nelson Mandela Metropolitan University, Port Elizabeth 6031, South Africa

\*Corresponding Author: email: [s207094248@live.nmmu.ac.za](mailto:s207094248@live.nmmu.ac.za);

Tel: 0415042255;

Fax: 0415041755

## Abstract

Cell mismatch occurs in Photovoltaic (PV) modules when a cell in a series connected string produces lower current than the other cells in that string. The current output of the string is limited by the weakest cell in the string. The effects of cell mismatch are visible in the current-voltage (I-V) characteristic curve of the module. Electroluminescence (EL) occurs in wavelength range of around 1000 to 1200 nm when a solar cell is forward biased and can be detected and imaged using a cooled CCD silicon camera. The EL signal intensity is related to cell performance and identifies material defects, bad contacts and broken cells.

In this study the cell mismatch in three single crystalline silicon modules was investigated. Two modules have visible degradation and signs of mechanical damage while the third module acts as a reference as it has no visible signs of damage. The I-V characteristic of the three modules was measured using outdoor I-V tracer equipment. The I-V curves indicate the presence of current mismatch in the degraded modules which is supported by the EL images of these modules. The EL images used, in conjunction with the I-V curves, allow the degradation in the modules to be characterised.

*Keywords: Photovoltaics, Cell Mismatch, Current-Voltage Characterisation, Electroluminescence*

## 1. Introduction

Photovoltaic (PV) technology has great potential as an alternative energy source. Cell Mismatch is a condition that arises from unbalanced current production of some cells in a series connected string. This mismatch results from degradation in the cell due to mechanically damaged cells or shading due to shadows or the accumulation of dirt [1]. Cell mismatch affects the current production of the cell and, hence, the string.

### 1.1. Current- Voltage (I-V) Characteristics and Cell Mismatch

The electrical performance of a PV module can be determined by measuring the current-voltage (I-V) characteristics using I-V tracer equipment. Cell mismatch has a substantial effect on the I-V curve of the whole module. A cell with a current output lower than the rest of the cells in the string is referred to as a "weak cell". When cells are connected in series the total current is limited by the weakest cell while the voltages add as normal. The weak cell in a series connection will become reverse biased with respect to the other cells and change from a power generator to a power dissipater [2]. The heat generated further damages the cell by creating a hot-spot which can cause the cell to crack or delaminate from the encapsulation material. The combined output of the series connected cells is dependent on the reverse voltage behaviour of the weak cell [3].

The effects of mismatch can be mitigated by using bypass diodes connected in parallel over a series connected cell or string of cells. The bypass diode is activated when the reverse bias in the weak cell or string of cells containing weak cells is equal to the transmission voltage of the diode [2]. The activation of the bypass diode results in a step in the I-V curve.

The relative position of the step in the I-V curve is related to the behaviour of the weak cell in reverse bias [3]. When cells are connected together to form modules it is impractical to have bypass diodes over each cell so they are connected over strings of series connected cells.

## **1.2. Electroluminescence**

Electroluminescence (EL) is a non destructive characterisation technique that provides spatial information about the solar cell material properties. This technique has been used to provide quantitative measurements of minority carrier lifetime, diffusion length [4][5][6] and series resistance [7]. The minority carrier diffusion length and lifetime are related to the collection efficiency of the cell material and is thus, an important material property.

EL occurs when a silicon solar cell is forward biased. The applied potential difference injects additional carriers into the junction. These carriers then move in the material until they recombine. The radiative recombination of carriers emits energy in the form of electromagnetic radiation, electroluminescence, in a range of 1000 to 1200 nm. The intensity of the EL signal is related to the material properties such as the surface recombination velocity, minority carrier lifetime and diffusion length [4]. Extrinsic defects that have occurred in the cell or module manufacturing process can also be detected.

EL signal is detected using a cooled charge-coupled device (CCD) camera which provides a greyscale spatial representation of defects in the cell. EL imaging easily identifies cell defects such as micro-cracks and finger defects.

## **1.3. Single Crystalline Silicon Modules**

Three single crystalline silicon modules were used in this investigation all with the same cell material and configuration. The modules have 44 cells connected in two strings of 22 cells with bypass diodes connected in parallel across the strings. The specified power output is 65W. Two of the modules have a visible grey-white discolouration that affects both modules to an equal extent. This is thought to be due to degradation in the anti-reflective coating on the cell surfaces. The effects of this degradation can be determined by comparing these modules with a third reference module that has no visible degradation.

## **1.4. Objectives:**

The objectives of this investigation are to identify and characterise cell mismatch in PV modules by comparing the results of the I-V characteristics with EL images. The EL images allow defective cells in a module to be identified and used to account for the decrease in output power observed.

## **2. Research methodology**

I-V curves were measured using a calibrated outdoor I-V tracer. The tracer equipment consists of a programmable power supply and an electronic load that allows the output current to be measured through a range of voltages. The current produced by the module is measured at each voltage point and this is plotted as the I-V curve of the module. The irradiance and the back-of-module temperature were measured while the I-V curve is measured. These were used to correct the results to standard operating conditions of 25°C and 1000 W/m<sup>2</sup>.

The I-V curve of the entire module was measured with and without bypass diodes. The I-V curves of the individual strings can also be measured allowing the current mismatch between the two strings to be identified. These I-V curves were measured for all three modules.

The EL image was measured by applying a forward bias of 30 V such that a current greater than the short circuit current of the module is applied. In this case approximately 4 A.

The wavelength of the emitted luminescence of a silicon sample has a peak at about 1150 nm and a portion of this peak can be detected by a Silicon CCD camera which has a detection range of 300-1000 nm. The CCD camera has a resolution of 3300 x 2500 pixels.. Cooling the CCD chip to -50 °C prevents noise in the signal due to dark currents. The data acquisition time is in the range of 1.5 to 2.5 seconds. The experimental set-up is illustrated in figure 1. The DC power supply provides the forward bias. In order for the electroluminescence signal to be detected the setup must be placed in a dark room as any other light source will affect the results. The CCD camera is connected to the computer where the Sensovation image processing software, which is supplied with the camera, is used to capture and analyse the images.

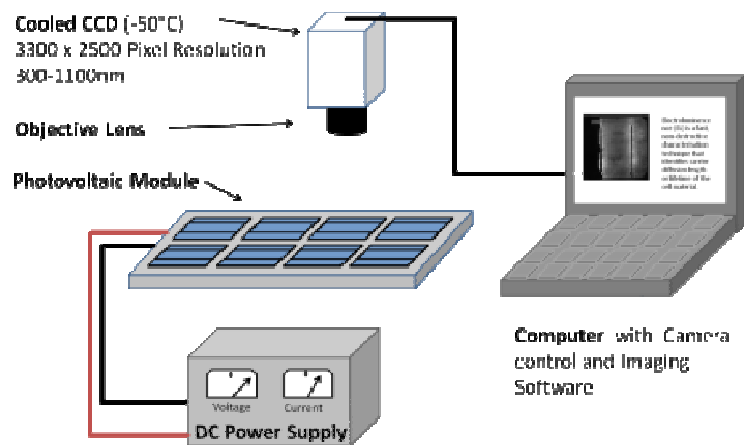


**Figure 1. Schematic outline of EL experimental setup**

Visual images of modules 1 and 2 and the reference module are shown in figure 2. The modules have a specified maximum power ( $P_{max}$ ) of 65 W, open circuit voltage ( $V_{oc}$ ) of 25 V and short circuit current ( $I_{sc}$ ) of 3.6 A.

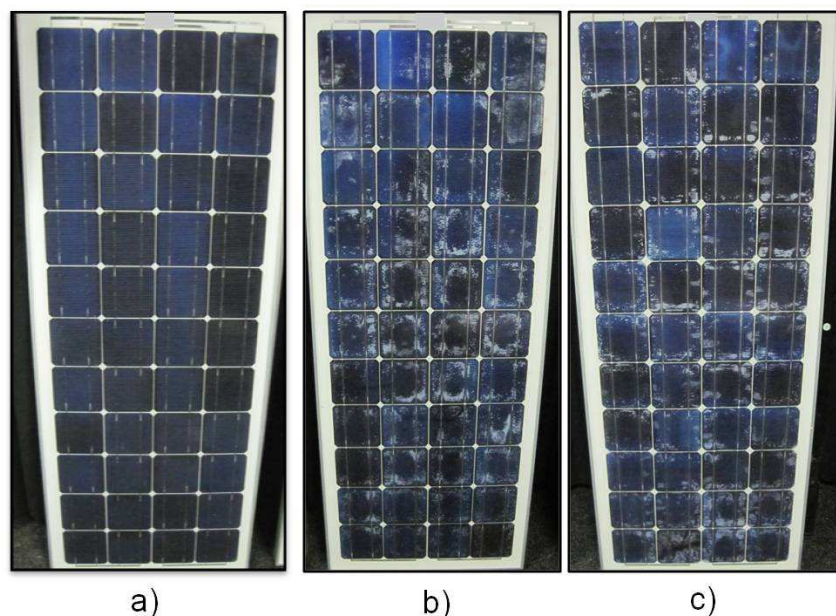


**Figure 2. Optical image of a) Module 1, b) Module 2 and c) Reference Module**

### 3. Results

#### 3.1. Reference Module

##### 3.1.1. I-V curves

The I-V curve of the reference module with bypass diodes and the individual strings is shown in figure 3. The I-V curve shows that the performance of the two strings is evenly matched. From the I-V curve it is clear that the voltages of the two strings add at equal currents, resulting in the I-V curve (blue) of the whole module which does not show any signs of mismatch.

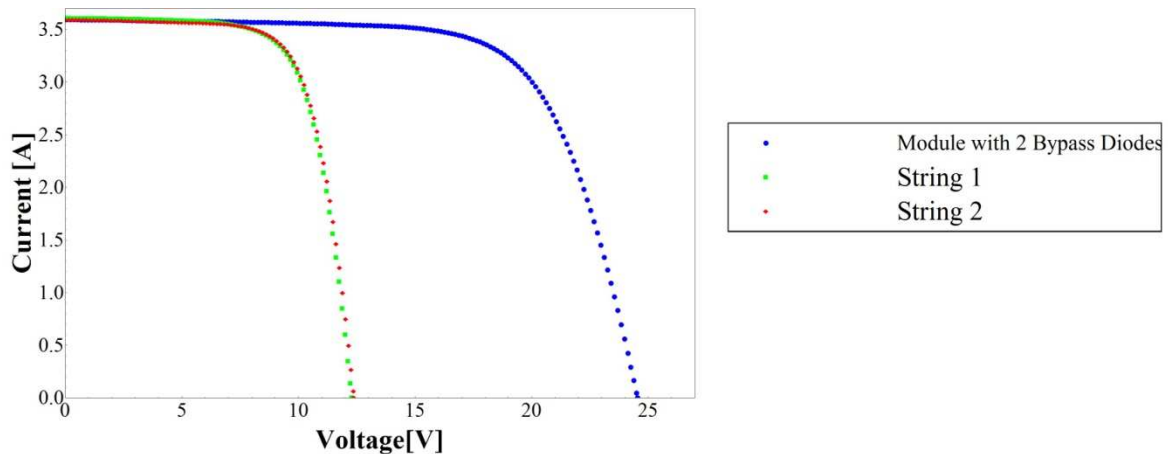


**Figure 3. I-V curves of reference module and the individual strings**

##### 3.1.2. EL images

The EL image of the reference module, figure 4(a), corroborates the results of the I-V curve as there are no large severely damaged areas visible and the two cell strings are evenly matched. Common cell defects that affect small areas can be detected in the module and are highlighted in figure 4(b).

Fingers are metallic contact areas that shade the cell and that run perpendicular to the busbars across the cell. Finger defects in the module are indicated in figure 4(b). A break across the finger results in the area between the fingers of the cell having decreased electrical contact. These defects are visible in the EL image as the area around the broken finger appears darker in the image. Finger defects occur in the majority of the cells in the module possibly due to problems in the manufacturing process.

Micro-cracks in the module are highlighted in figure 4(b). Silicon solar cells are made of thin fragile wafers, the occurrence of micro-cracks is fairly common. Micro-cracks can occur in the manufacturing process of the cell but more frequently in assembly process of the module.

The effect of these cracks on the module power output depends on the extent of the cracks and whether the cracks prevent portions of the cells from achieving electrical contact. A crack in the cell material prevents electrical contact to the area and results in either fewer carriers being generated or none at all. The resulting lack of radiative recombination in these areas causes these defects to have a lower intensity EL signal than the rest of the cell. The micro-cracks indicated by label (ii) are visible in the EL but do not cause inactive areas in the cells. These cracks have a minimal effect on the performance on the module. The micro-crack labelled (iii) completely removes areas of the cell from electrical contact which appear completely dark in the EL image. This inactive area indicates that this area of the cell has poor photoresponse lowering the performance of the cell. It has been

shown that with time and thermal cycling micro-cracks can become more serious and result in inactive areas [9], which, in turn, results in performance degradation.

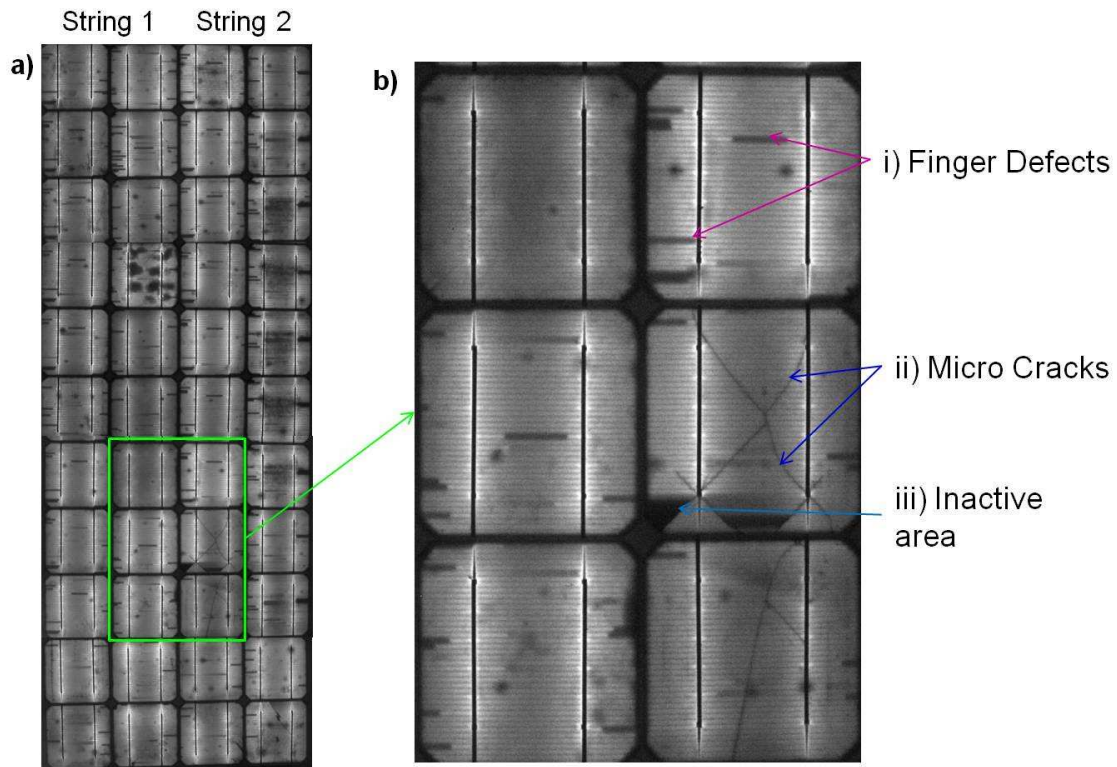


**Figure 4. The EL image of (a) the entire reference module with (b) a section enlarged to illustrate common cell defects**

### 3.2. Module 1

#### 3.2.1. I-V curves

The I-V curve of module 1 and the cell strings is shown in figure 5. String 1 has a lower  $I_{sc}$  and power output than string 2. This results in current mismatch between the two strings which causes the bypass diode across string 1 to be activated. The step in the I-V curve of the module is due to the activation of the bypass diode resulting from the reverse bias behaviour of the damaged cells.

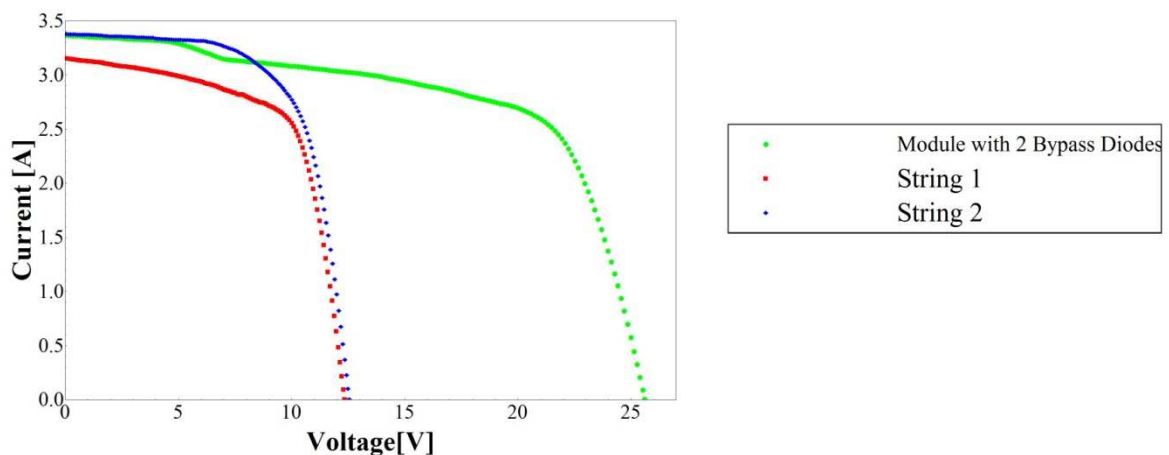


**Figure 5. I-V curve of Module 1 and the individual strings.**

### 3.2.2. EL images

The EL image of this module is seen in figure 6(a) with several defects highlighted and enlarged in figures 6(b), (c) and (d).

In figure 6(b) the effect of the degradation in the anti-reflective coating is visible in the EL image. Areas that have been discoloured correspond with areas of lower EL signal intensity. This could mean that the cell material in these regions is damaged or that the discolouration of the coating blocks the EL signal from being detected. Either way this degradation results in poor photo-response and, ultimately, performance degradation in the affected areas.

Figure 6(c) highlights a cell where a micro-crack has prevented electrical contact between the one side of the cell and the other. The high current density in the one third of the cell results in a higher intensity EL signal.

Figure 6(d) highlights the area of the module where several cells and been cracked. These cracks cause large inactive areas which result in lower performance of these cells. The cause of this damage is most likely due to mechanical damage as the cracks line up with scratches that have been observed along the back surface of the module.

The EL images explain the mismatch seen in the two strings as there are more damaged cells in string 1 than in string 2.

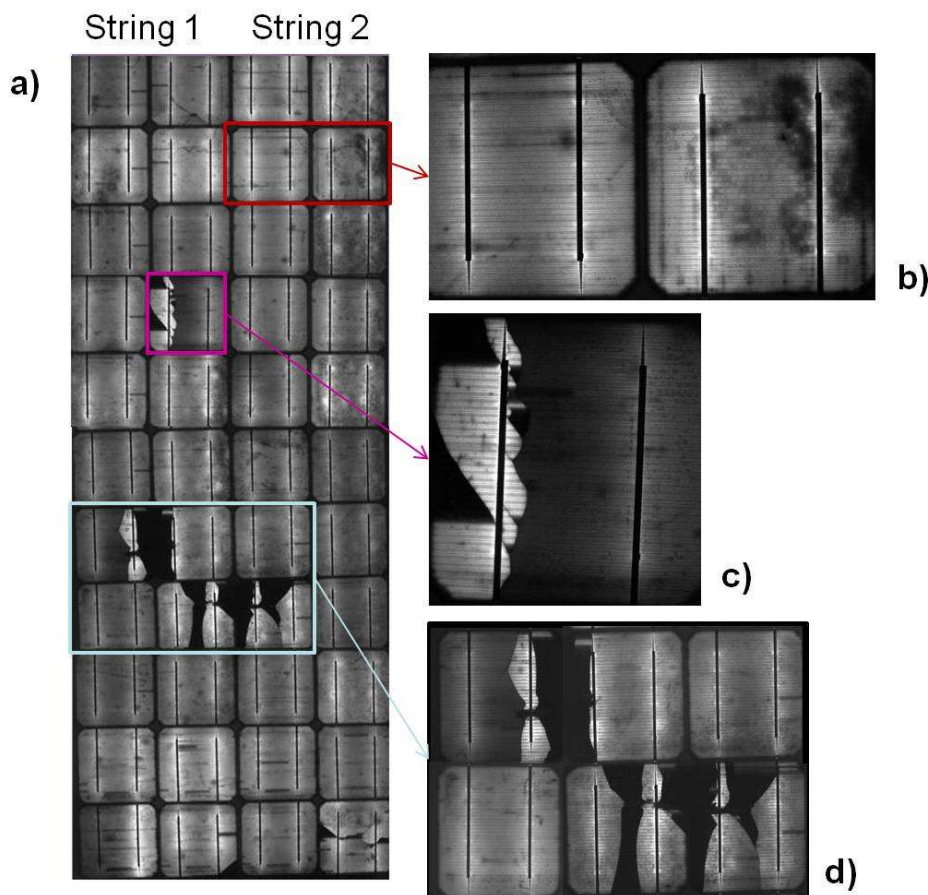


**Figure 6. The EL image of (a) module 1 with EL images of defects enlarged b) degradation of anti-reflective, c) micro-cracks resulting in high current density and d) micro-cracks resulting in inactive areas**

### 3.3. Module 2

#### 3.3.1. I-V curve

The I-V curve of module 2 and the individual strings is shown in figure 7. The strings both have similar current output but the shape of the I-V curve of string 1 indicates the significant influence of the shunt resistance of one string on the I-V curve of the module. In an ideal solar cell the shunt resistance is infinite. The shunt resistance results in the slope of the graph changing in the region between short circuit and the maximum power point or “knee” of the I-V curve.

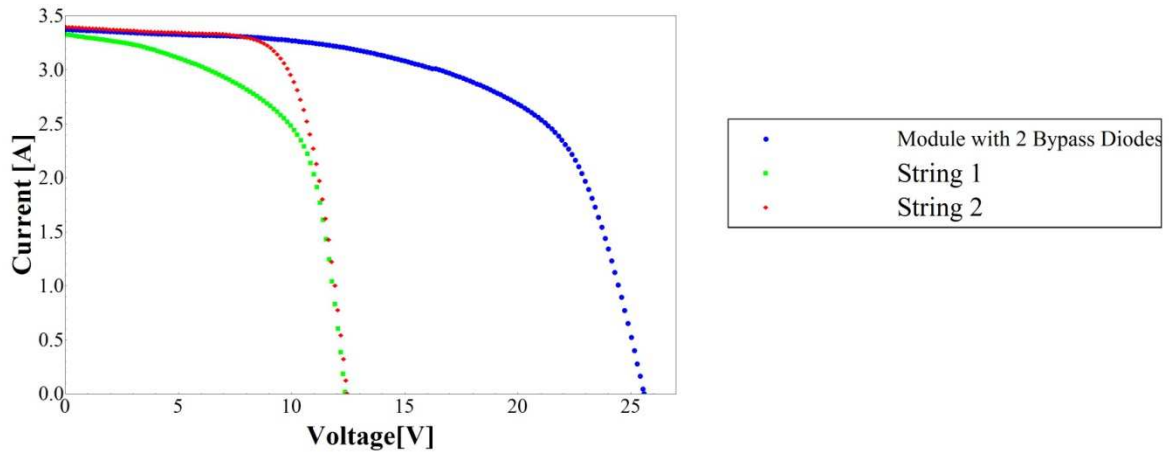


Figure 7. I-V curve of module 2 and the individual strings

#### 3.3.2. EL images

The EL image of module 2 is shown in figure 8(a). Highlighted in the figure 8(b) is the most damaged cell in the module. This cell has cracks which result in large inactive areas which lower the performance of the module. The I-V curve of the string containing this cell suggests that the damage to this cell results in lowering of the shunt resistance of the cell, causing more photo generated current to bypass the cell’s diode junction.

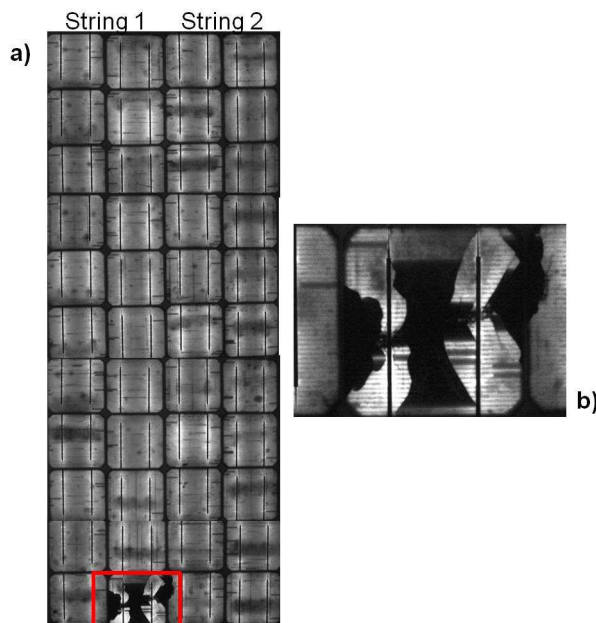
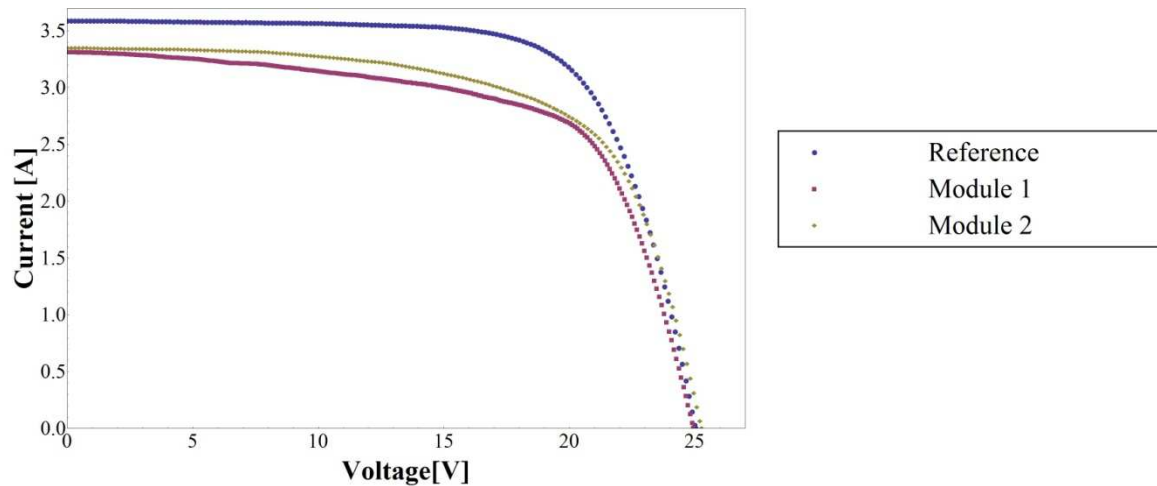


Figure 8. The EL image of the (a) entire module 2 with (b) the most damaged cell highlighted

### 3.4. Comparison of performance of modules

Figure 9 shows the I-V curves of the 3 modules compared without the bypass diodes included in the configuration. The reference module has the best power and current output as expected and has a measured  $P_{max}$  of 63W. The variation from the specified 65W is due to the defects that were only visible in the EL image.

The I-V curves of module 1 and 2 look very similar even though module 1 has a greater number of severely cracked cells. Since these I-V curves were taken without bypass diodes the current output is limited by the weakest cell in each string and this implies that the weakest cell in both modules have a similarly poor photo-response.



**Figure 9. The I-V curves of modules 1 and 2 and the reference module without bypass diodes**

## 4. Conclusions

Electroluminescence is a fast and effective technique in identifying defects and degradation in PV modules. It is able to quickly detect cell defects that would not be detected in visual module inspections. These defects can account for a decrease in the module performance in a module that would otherwise appear to be undamaged like the reference module. Defects in a module can be detected at the manufacturing stage enabling manufacturers to increase the reliability of PV modules. Cell mismatch can be observed in the I-V curves of a module but the EL image of the module allows the identification of cells and the exact nature of the defects to be determined.

The EL images of module 1 clearly indicate the causes of the cell mismatch which is seen in the I-V curve of the module. The cracked cells and inactive areas in one string result in a lower current output and lower shunt resistance which is visible in the I-V curve. Similarly a damaged cell in module 2 results in a lower current output and shunt resistance visible in the I-V curve of the module.

Collaboration between the I-V characterisation and EL imaging allows the lower power outputs of the module compared to the manufactures specification to be fully explained.

## References

- [1] Meyer E.L., van Dyk E.E., 2004. Assessing the reliability and degradation of photovoltaic module performance parameters, *IEEE Transactions on Reliability* 53, p.83-92.
- [2] Vorster F.J., van Dyk E.E., 2005. Current-Voltage characteristics of high-concentration, photovoltaic arrays, *Progress in Photovoltaics: Research and Applications* 13, 55-66.
- [3] Alonso-Garcia M.C., Rui J.M., 2006. Analysis and modelling the reverse characteristic of photovoltaic cells, *Solar Energy Materials & Solar Cells* 90, 1105–1120.
- [4] Fuyuki T., Kondo H., Yamazaki T., Takahashi Y., Uraoka Y., 2005. Photographic surveying of minority carrier diffusion length in polycrystalline silicon solar cells by electroluminescence, *Applied Physics Letters* 86, 262108.
- [5] Fuyuki T., Kondo H., Kaji Y., Ogane A., Takahashi Y., 2007. Analytic findings in the electroluminescence characterization of crystalline silicon solar cells, *Journal of Applied Physics* 101, 023711.
- [6] Würfel P., Trupke T., Puzzer T., Schäffer E., Warta W, Glunz S.W., 2007. Diffusion lengths of silicon solar cells from luminescence images, *Journal of Applied Physics* 101, 123110.
- [7] Hinken D., Ramspeck K., Bothe K., Fischer B., Brendel R., 2007. Series resistance imaging of solar cells by voltage dependent electroluminescence, *Applied Physics Letters* 91, 182104.
- [8] Fuyuki T., Kitiyanan A., 2009. Photographic diagnosis of crystalline silicon solar cells utilizing Electroluminescence, *Applied Physics A*. 963, 189-196.
- [9] Köntges M., Kunze I., Kajari-Schröder S., Breitenmoser X., Bjørneklett B., 2011. The risk of power loss in crystalline silicon based photovoltaic modules due to micro-cracks, *Solar Energy Materials & Solar Cells* 95, 1131–1137.